Article:

Ismail, M.S., Ingham, D.B., Hughes, K.J. et al. (2 more authors) (2016) The effects of shape on the performance of cathode catalyst agglomerates in polymer electrolyte fuel cells: a micro-scale FEM study. International Journal of Numerical Methods for Heat and Fluid Flow, 26 (3/4). pp. 1145-1156. ISSN 1758-6585

https://doi.org/10.1108/HFF-10-2015-0416

The effects of shape on the performance of cathode catalyst agglomerates in polymer electrolyte fuel cells: a micro-scale FEM study

Journal:	*International Journal of Numerical Methods for Heat and Fluid Flow*
Manuscript ID	HFF-10-2015-0416.R1
Manuscript Type:	Research Article
Keywords:	Finite element method, Transport phenomena, Agglomerate shape, Agglomerate model, Cathode catalyst layer, Polymer electrolyte fuel cells

Abstract

Purpose – This paper aims to numerically investigate the effects of the shape on the performance of the cathode catalyst agglomerate used in polymer electrolyte fuel cells (PEFCs). The shapes investigated are slabs, cylinders and spheres.

Design/methodology/approach – Three 1D models are developed to represent the slab-like, cylindrical and spherical agglomerates, respectively. The models are solved for the concentration of the dissolved oxygen using a finite element software, COMSOL Multiphysics®. '1D' and '1D axisymmetric' schemes are used to model the slab-like and cylindrical agglomerates respectively. There is no one-dimensional scheme available in COMSOL Multiphysics® for spherical coordinate systems. To resolve this, the governing equation in '1D' scheme is mathematically modified to match that of the spherical coordinate system.

Findings – For a given length of the diffusion path, the variation in the performances of the investigated agglomerates is dependent on the operational over-potential. Under low magnitudes of the over-potentials, where the performance is mainly limited by reaction, the slab-like agglomerate outperforms the spherical and cylindrical agglomerates. In contrast, under high magnitudes of the over-potentials where the agglomerate performance is mainly limited by diffusion, the spherical and cylindrical agglomerates outperform the slab-like agglomerate.

Practical implications – The current advances in the nano-fabrication technology gives more flexibility in designing the catalyst layers in PEFCs to the desired structures. If the design of the agglomerate catalyst is to be assessed, the current micro-scale modelling offers an efficient and rapid way forward.

Originality/value – The current micro-scale modelling is an efficient alternative to developing a full (or half) fuel cell model to evaluate the effects of the agglomerate structure.

Keywords: Finite element method, Transport phenomena, Agglomerate shape, Agglomerate model, Cathode catalyst layer, Polymer electrolyte fuel cells.

1. Introduction

Over the last few years, there has been worldwide concern over the environmental and health-related consequences of the use of fossil fuels to produce useful energy. The combustion of fossil fuels releases harmful emissions into the atmosphere that adversely affect both the environment and the health of human beings. Therefore, the world as whole is driven towards adopting and developing cleaner power sources. Within this context, polymer electrolyte fuel cells (PEFCs) have been very promising zero/low emission power sources; this is mainly due to their relatively high efficiency and low temperature start-up (Mench, 2008). However, there are still some technical and economic challenges that need to be addressed to allow a wider emergence of PEFC technology into the marketplace. One of the main challenges is the slow rate of the oxygen reduction reaction (ORR) takes place at the cathode electrode. This slow reaction rate manifests itself through the high activation losses presented by the cathode electrode. In order to have insights on how to improve the performance of the cathode catalyst layer, a better understating of the physics taking place in this layer should be gained. At the same time, the cathode catalyst layer is the least understood layer in PEFCs and this is due to the highly-coupled and complex physics taking place at this layer (Yoon and Weber, 2011). Due to the prohibitive cost and time-consuming nature of the relevant experiments, mathematical and computational modelling is a cost-effective and efficient alternative approach to better understand the physics taking place at the cathode catalyst layer.

There are mainly two approaches to treat the catalyst layer in the modelled PEFC. The first approach models the catalyst layer as an interface at which the source and sink terms are set; see for example (Berning et al., 2002; Berning and Djilali, 2003). In the second approach, the catalyst layer is modelled as a volume in which the various transport phenomena take place.

The models under this approach are normally classified as what are known as homogeneous models and agglomerate models. The homogenous models assume that the catalyst layer is a porous layer that consist of a homogenous (i.e. uniform) mixture of the ionomer, platinum and carbon; see for example (Kulikovsky et al., 1999; Meng and Wang 2004; Song et al., 2004; Um and Wang, 2004; Zhou and Liu, 2004; Carcadea, et al., 2007; Hasan et al., 2011; Ismail et al., 2012). The agglomerate models also assumes that the catalyst layer is a porous layer that consists of a uniform mixture of the ionomer, carbon and platinum; however, these models are more realistic as they (i) account for the dissolution of oxygen into the ionomer phase, and (ii) capture, to a certain extent, the microstructure of the catalyst layer. Some agglomerate models have been described in Broka and Ekdunge (1997), Jaouen et al. (2002), Siegel et al. (2003), Wang et al. (2004), Sun, et al. (2005), Yin (2005), Madhusudana and Rengaswamy (2006), Secanell et al. (2007), Kamarajugadda and Mazumder (2008), Jain, et al. (2010), Obut and Alper (2011), Tabe et al. (2011), Yoon and Weber (2011), Kamarajugadda and Mazumder (2012), Moein-Jahromi and Kermani (2012), Cetinbas et al. (2013), Cetinbas, Advani et al. (2014) and Ismail et al. (2015).

In the agglomerate models, the catalyst layer is normally assumed to consist of spherical and isolated agglomerates of uniform composition of catalyst and ionomer particles, and covered by a thin ionomer layer (Ismail et al., 2015).The spherical shape of the agglomerates has been supported by the micrographs of the catalyst layer; however, these micrographs have also shown that these agglomerates tend not to be isolated but overlapping with each other (Kamarajugadda and Mazumder, 2012). Kamarajugadda and Mazumder (2012) showed that when the agglomerate size is small (< 200 nm), the effect of the agglomerate shape is insignificant. For larger agglomerates (600-1000 nm), a better performance was obtained with overlapping agglomerates than a single agglomerate with the same volume. With the advancement in the nano-fabrication technology, it will be possible to engineer the fuel cell catalyst layers to the desired structures (Kamarajugadda and Mazumder, 2012). Jain et al. (2010) numerically investigated the effects of the shape of the agglomerate with the shapes investigated being plate-like, spherical and cylindrical. The best performance was obtained by the modelled fuel cell with the spherical agglomerates, but, almost the same limiting current density was obtained by all the modelled fuel cells. Marthosa (2012) developed a one-dimensional model for a PEFC cathode electrode and found that, maintaining the volume of the agglomerate constant, the cathode electrode performs better with thin and long cylindrical and slab-like agglomerates.

To the best of the author's knowledge, the above three investigations, i.e. Jain et al. (2010), Kamarajugadda and Mazumder (2012) and Marthosa (2012), are the only ones that have investigated the effects of the shape of the agglomerate. In this work, we investigate the effects of the shape of the catalyst agglomerate on the performance of that agglomerate. The agglomerate has been assumed to take one of the following common shapes: slab-like, cylindrical and spherical. The investigation of the design effects at this microscale level is efficient as the over-potential within the active region of the agglomerate is almost constant and therefore the conservation of charge equations do not need to be solved. Subsequently, if the design of the agglomerate is investigated, the current micro-scale modelling offers an efficient alternative to the full (or half) fuel cell models, which involves complex physics and, consequently, require much more computational time.

2. Model formulation

Three one-dimensional models have been developed for agglomerates with three different shapes: slab-like, cylindrical and spherical. To neglect the end effects, the slab-like and cylindrical agglomerates were assumed to be semi-infinite (Rawlings and Ekerdt, 2002). Also, each agglomerate was assumed to consist of an active region, where the reaction takes place, and ionomer film covering this active region. The active region is made up from a uniform mixture of the ionomer, carbon and platinum which provide pathways for protons, dissolved oxygen and electrons to meet and react. A schematic of the computational domain of the modelled agglomerates is shown in Figure 1.

Due to the very small scale of the geometry modelled and the relatively high thermal, electrical and ionic conductivity values of the agglomerate material, the model is assumed to be isothermal, and iso-potential (electrically and ionically). Also, the fuel cell was assumed to operate under low-humidity conditions in order not to obscure the results with not fully–understood two phase phenomena (Yoon and Weber, 2011). Therefore, the only equation solved in the model is the mass transport of oxygen:

$$\nabla D_e^{eff} \nabla C_{O_2} + R_{O_2} = 0 \qquad (1)$$

where C_{O_2} is the molar concentration of the dissolved oxygen and D_e^{eff} is the effective diffusivity of the dissolved oxygen in the ionomer phase and is given as follows (Sun, et al., 2005):

$$D_e^{eff} = \begin{cases} D_e & in\ the\ ionomer\ film \\ \varepsilon_e^{1.5} D_e & in\ the\ active\ region \end{cases} \qquad (2)$$

where D_e is the diffusivity of the dissolved oxygen in the pure ionomer and ε_e is the volume fraction of the ionomer phase in the active region. R_{O_2} is the oxygen molar consumption rate and is obtained as follows (Yoon and Weber, 2011):

$$R_{O_2} = \begin{cases} 0 & \text{in the ionomer film} \\ -kC_{O_2} & \text{in the active region} \end{cases} \tag{3}$$

$$k = \frac{i_o a}{4FC_{O_2}^{ref}} \exp\left(\frac{-\alpha F}{RT}\eta\right) \tag{4}$$

where k is the reaction rate constant, i_o is the exchange current density, F is the Faraday's constant, $C_{O_2}^{ref}$ is the reference concentration of the dissolved oxygen, α is the charge transfer coefficient, T is the temperature, R is the universal gas constant and η is the activation over-potential which is the input variable of the model. a is the specific area of the platinum catalyst, i.e. surface area of platinum per unit volume of the that catalyst, and is given by (Yoon and Weber, 2011):

$$a = \frac{l_{pt} A_{pt}}{L_{cl}} \tag{5}$$

where l_{pt} is the platinum loading, A_{pt} is the electrochemical surface area of the platinum catalyst and L_{cl} is the thickness of the catalyst layer.

It should be noted that each shape investigated should be solved in its appropriate coordinate system, namely Cartesian coordinate system from slabs, cylindrical coordinate system for cylinders and spherical coordinate system for spheres. Therefore, the one-dimensional Equation (1) takes the following forms in the various coordinate systems:

$$\nabla D_e^{eff} \nabla C_{O_2} + R_{O_2} = \begin{cases} \dfrac{d}{dx}\left(D_e^{eff} \dfrac{dC_{O_2}}{dx} \right) + R_{O_2} & \textit{Cartesian coordinate system} \\ \dfrac{1}{r}\dfrac{d}{dr}\left(r D_e^{eff} \dfrac{dC_{O_2}}{dr} \right) + R_{O_2} & \textit{Cylinderical coordinate system} \\ \dfrac{1}{r^2}\dfrac{d}{dr}\left(r^2 D_e^{eff} \dfrac{dC_{O_2}}{dr} \right) + R_{O_2} & \textit{Spherical coordinate system} \end{cases} \quad (6)$$

The boundary conditions used are a specified concentration at the surface of the ionomer film and symmetry at the centre of the agglomerate; see Figure 1. The specified concentration at the surface of the ionomer film is given by Henry's law (Sun, et al., 2005):

$$C_{O_2,o} = \frac{C_{O_2,g} RT}{H} \quad (7)$$

where $C_{O_2,g}$ is the concentration of the gaseous oxygen at the surface of the ionomer film (it was assumed to be that of the flow channel) and H is the Henry's constant. It should be noted that, since a single computational domain is used, the continuity in the flux of the dissolved oxygen at the interface between the ionomer film and the active region is ensured.

[Insert Figure 1]

Equation (1) was solved using a finite element software, COMSOL Multiphysics® 5.1. The computational domain was discretised and refined, especially near to the interface between the ionomer film and the active region, until a mesh independent solution is obtained. Figure 2 shows the normalised concentration of oxygen in the slab-like agglomerate near the interface between the ionomer film and the active region at an over-potential of -0.8 V, where the variation in concentration is relatively high. It is clear that the solution becomes mesh-independent with 72 elements; further refinement does not result in further improvement. Figure 3 shows the distribution of the elements in the regions next to the interface between the ionomer film and active region for the 72-elemnet mesh. It is clear that the size of the elements grow exponentially away from the interface. Table 1 shows the physical parameters used for the model.

[Insert Figure 2, Figure 3 and Table 1]

Before concluding this section, it should be noted that, for one-dimensional models, Cartesian coordinate and cylindrical coordinate systems are used when selecting '1D' and '1D Axisymmetric' schemes respectively in COMSOL Multiphysics®. However, there is no one-dimensional scheme available in COMSOL Multiphysics® for spherical coordinate systems. To resolve this, Equation (6) in the Cartesian coordinate system (i.e. in the '1D' scheme) was mathematically modified to match that of the spherical coordinate system. It should be noted that the modified equation was multiplied by 'r^2' to avoid dividing by zero. More details on this technique is available in the application 'Spherically Symmetric Transport' available in the COMSOL Application Libraries.

3. Results and discussion

In order to examine the reliability of the numerical model, it is a good practice to compare the numerical solution of the computational model to the analytical solution if the latter is available. Equation (1) has been solved analytically for all the shapes investigated in this paper (Aris, 1957; Fogler, 2006; Moein-Jahromi and Kermani, 2012). As an example, considering the boundary conditions shown in Figure 1, the analytical solution for the concentration of oxygen in the spherical agglomerate (without an ionomer film) is given as follows (Moein-Jahromi and Kermani, 2012):

$$C_{O_2} = C_{O_2,s}\left(\frac{R_a}{r}\right)\left(\frac{\sinh\left(3(r/R_a)\Phi\right)}{\sinh\left(3\Phi\right)}\right) \tag{8}$$

where $C_{O_2,s}$ is the concentration of oxygen at the surface of the agglomerate, R_a is the radius of the agglomerate and Φ is the Thiele modulus which is, in the case of spheres, given as follows:

$$\Phi = \frac{R_a}{3}\sqrt{\frac{k}{D_e^{eff}}} \tag{9}$$

where k and D_e^{eff} are the reaction rate constant and effective diffusivity, respectively, of the dissolved oxygen in the ionomer; they both have been defined in the previous section. It should be noted that the solution shown in Equation (8) is for a spherical agglomerate without an ionomer film. In order to compare the analytical and numerical solutions, the ionomer film was, for this purpose, discarded from the computational domain. In other words, only the active region of the agglomerate was modelled and numerically solved. Figure 4 shows the analytical and numerical solution of the distribution concentration in a spherical agglomerate at some Thiele Moduli. It is clear that the agreement between the two solutions is excellent.

[Insert Figure 4]

Subsequently, the one-dimensional models for the agglomerates with various shapes were solved. Figure 5 shows the concentration profiles of the modelled agglomerates at various over-potentials, namely -0.2, -0.3, -0.4, -0.5, -0.6, -0.7 and -1.0 V. It can be seen from the figure that the amounts of the present (or unreacted) oxygen at low over-potentials of -0.2 and - 0.3 V are higher in the spherical and cylindrical agglomerates than that in slab-like agglomerate. In other words, the amount of the reacted oxygen in the slab-like agglomerate is higher than those in the spherical and cylindrical agglomerates in the low over-potential magnitudes where the performance of the agglomerate is mainly limited by reaction. However, as the magnitude of the over-potential increases, the variations in the profiles of the unreacted oxygen of the agglomerates becomes less, especially after -0.5 V over-potential where the performance of the agglomerate becomes increasingly limited by the diffusion of the dissolved oxygen. It is worth to note that at -1.0 over-potential, the rate of consumption of the dissolved oxygen is so high that the dissolved oxygen completely reacts as soon as it enters the active region of the agglomerate, thus giving rise to what is known as a limiting current density.

[Insert Figure 5]

The performance for each agglomerate, in the form of polarisation curve was then computed, see Figure 6. The current density, i, for the various investigated agglomerates was calculated as follows:

$$i = \begin{cases} \int_0^{L_{agg}} 4FR_{O_2}\,dx \quad \textit{for slab-like agglomerate} \\ \frac{1}{L_{agg}} \int_0^{L_{agg}} 4FR_{O_2}\,r\,dr \quad \textit{for cylinderical agglomerate} \\ \frac{1}{L_{agg}^2} \int_0^{L_{agg}} 4FR_{O_2}\,r^2\,dr \quad \textit{for spherical agglomerate} \end{cases} \qquad (10)$$

[Insert Figure 6]

Figure 6 shows that the slab-like agglomerate performs better than the cylindrical and spherical agglomerates in the low current density region, i.e. < 800 A m^{-2}. This superiority in performance, demonstrated by the slab-like agglomerate in this region, can be explained by re-visiting Figure 5. Under low magnitudes of over-potentials where the performance is mainly limited by reaction, the latter figure shows that the amount of the reacted oxygen, which is proportional to the electric current generated, in the slab-like agglomerate is higher than those in the cylindrical and spherical agglomerates. In contrast, in the high current density region where the performance of the agglomerate is mainly limited by diffusion, i.e. > 1300 A m^{-2}, the spherical and cylindrical agglomerates outperform the slab-like agglomerate. This is due to the better diffusion of the dissolved oxygen in the spherical and cylindrical agglomerates. Finally, in the intermediate current density region, i.e. between 800 and 1300 A m^{-2}, all the agglomerates perform almost the same and this is due to the performance being equally limited by the reaction and diffusion in this region.

As a final note, it should be noted that in this investigation the diffusion path of the active region rather than the characteristic length, which is defined as the ratio between the volume of the ionomer film-free agglomerate and its external surface area (Aris, 1957), was selected to be the same for all the agglomerates investigated (i.e. 1 μm). This selection was made in order to have a direct comparison of the concentration profiles of all the investigated agglomerates and to avoid the uncertainty arising from whether the ionomer film should remain the same for the all the agglomerates or should be proportional to the size of the characteristic length of each agglomerate.

4. Conclusions and future work

The sensitivity of the performance of the PEFC catalyst agglomerate to its shape has been numerically investigated in this paper. The shapes investigated are slabs, cylinders and spheres. A one-dimensional model has been developed for each agglomerate and solved using finite element software, COMSOL Multiphysics®. The effects of the agglomerate shape has been demonstrated through generating the polarisation curve for each agglomerate investigated. The following are the main conclusions:

- The slab-like agglomerate outperforms the spherical and cylindrical agglomerates in the low current density region where the performance is mainly limited by the reaction of oxygen.
- The spherical and cylindrical agglomerate outperform the slab-like agglomerate in the high current density region where the performance is mainly limited by the diffusion of the dissolved oxygen.
- In the intermediate current density region, the performance of all the investigated agglomerates are almost the same and this is mainly due to the performance being equally limited by reaction and diffusion.

The next logical step is to investigate the sensitivity of the modelled fuel cell performance to the shape of the agglomerate. The initial results of the respective models confirm the main findings obtained in the present work at the micro-scale level.

Nomenclature

a	Specific area of platinum catalyst	m^{-1}
A_{pt}	Electrochemical surface area of catalyst	m^2
C_{O_2}	Concentration of dissolved oxygen	mol m^{-3}
$C_{O_2,g}$	Concentration of gaseous oxygen	mol m^{-3}
$C_{O_2}^{ref}$	Reference concentration of dissolved oxygen	mol m^{-3}
D_e	Oxygen diffusivity in the ionomer	m^2 s^{-1}
F	Faraday's constant	C mol^{-1}
H	Henry's constant for oxygen in the ionomer	atm m^3 mol^{-1}
i	Current density	A m^{-2}
i_o	Exchange current density	A m^{-2}
k	Reaction rate constant	s^{-1}
l_{pt}	Platinum loading	m
L_{agg}	Diffusion path of the active region	m
L_{cl}	Thickness of catalyst layer	m
p	Pressure	Pa
R	Universal gas constant	J K^{-1} mol^{-1}
R_{O_2}	Molar consumption rate of oxygen	mol m^{-3} s^{-1}
T	Temperature	K

Greek symbols

α	Charge transfer coefficient	-
ε_e	Volume fraction of ionomer	-
η	Overpotential	V
Φ_L	Thiele modulus	-

References

Aris, R. (1957), "On shape factors for irregular particles—I: The steady state problem. Diffusion and reaction", *Chemical Engineering Science*,Vol. 6 No. 6, pp. 262-268.

Berning, T. and Djilali, N. (2003), "A 3D, Multiphase, Multicomponent Model of the Cathode and Anode of a PEM Fuel Cell", *Journal of The Electrochemical Society*, Vol. 150 No. 12, pp. A1589-A1598.

Berning, T., Lu, D.M. and Djilali, N. (2002), "Three-dimensional computational analysis of transport phenomena in a PEM fuel cell", *Journal of Power Sources*, Vol. 106 No. 1–2, pp. 284-294.

Broka, K. and Ekdunge, P. (1997), "Modelling the PEM fuel cell cathode", *Journal of Applied Electrochemistry*, Vol. 27 No. 3, pp. 281-289.

Carcadea, E., Ene, H., Ingham, D.B., Lazar, R., Ma , L., Pourkashanian, M. and Stefanescu, I. (2007), "A computational fluid dynamics analysis of a PEM fuel cell system for power generation" *International Journal of Numerical Methods for Heat & Fluid Flow*, Vol. 17 No. 3, pp. 302-312.

Cetinbas, F. C., Advani, S.G. and Prasad, A.K. (2013), "A Modified Agglomerate Model with Discrete Catalyst Particles for the PEM Fuel Cell Catalyst Layer", *Journal of The Electrochemical Society*, Vol. 160 No. 8, pp. F750-F756.

Cetinbas, F.C., Advani, S.G. and Prasad, A.K. (2014), "Three dimensional proton exchange membrane fuel cell cathode model using a modified agglomerate approach based on discrete catalyst particles", *Journal of Power Sources*, Vol. 250, pp. 110-119.

Fogler, H.S. (2006), "Elements of Chemical Reaction Engineering", Chapter 12. New Jersey Pearson Education.

Hasan, A.B.M., Wahab, M.A., Guo, S.M., (2011), "CFD analysis of a PEM fuel cell for liquid dispersion at the interface of GDL-GFC", International Journal of Numerical Methods for Heat & Fluid Flow, Vol. 21 No. 7, pp. 810 - 821

Ismail, M.S., Hughes, K.J., Ingham, D.B., Ma, L. and Pourkashanian, M. (2012) "Effects of anisotropic permeability and electrical conductivity of gas diffusion layers on the performance of proton exchange membrane fuel cells", Applied Energy, Vol. 95, pp. 50-63.

Ismail, M.S., Hughes, K.J., Ingham, D.B., Ma, L. and Pourkashanian, M. (2015), "Effective diffusivity of polymer electrolyte fuel cell gas diffusion layers: An overview and numerical study", International Journal of Hydrogen Energy, Vol. 40 No. 34, pp. 10994-11010.

Jain, P., Biegler, L.T. and Jhon, M.S. (2010), "Sensitivity of PEFC Models to Cathode Layer Microstructure" Journal of The Electrochemical Society, Vol. 157 No. 8, pp. B1222-B1229.

Jaouen, F., Lindbergh, G. and Sundholm, G. (2002), "Investigation of Mass-Transport Limitations in the Solid Polymer Fuel Cell Cathode: I. Mathematical Model", Journal of The Electrochemical Society, Vol. 149 No. 4, pp. A437-A447.

Kamarajugadda, S. and Mazumder, S. (2008), "Numerical investigation of the effect of cathode catalyst layer structure and composition on polymer electrolyte membrane fuel cell performance", Journal of Power Sources, Vol. 183 No. 2, pp. 629-642.

Kamarajugadda, S. and Mazumder, S. (2012), "Generalized flooded agglomerate model for the cathode catalyst layer of a polymer electrolyte membrane fuel cell", Journal of Power Sources, Vol 208, pp. 328-339.

Kulikovsky, A.A., Divisek, J. and Kornyshev, A.A. (1999), "Modeling the Cathode Compartment of Polymer Electrolyte Fuel Cells: Dead and Active Reaction Zones" *Journal of The Electrochemical Society*, Vol. 146 No. 11, pp. 3981-3991.

Marthosa, S. (2012). "Improvement of electrocatalyst performance in hydrogen fuel cells by multi-scale modelling", Chapter 6, PhD Thesis, University of Manchetser.

Madhusudana, R.R. and Rengaswamy, R. (2006), "Dynamic characteristics of spherical agglomerate for study of cathode catalyst layers in proton exchange membrane fuel cells (PEMFC)" *Journal of Power Sources*, Vol. 158 No.1, pp. 110-123.

Mench, M.M. (2008), "Fuel Cell Engines", Chapter 1, Hoboken, John Wiley & Sons.

Meng, H. and Wang, C.Y. (2004), "Electron Transport in PEFCs", *Journal of The Electrochemical Society*, Vol 151 No 3, pp. A358-A367.

Moein-Jahromi, M. and Kermani M.J. (2012), "Performance prediction of PEM fuel cell cathode catalyst layer using agglomerate model", *International Journal of Hydrogen Energy*, Vol. 37 No. 23, pp. 17954-17966.

Obut, S. and Alper, E. (2011), "Numerical assessment of dependence of polymer electrolyte membrane fuel cell performance on cathode catalyst layer parameters", *Journal of Power Sources*, Vol. 196 No. 4, pp. 1920-1931.

Rawlings, J.B. and Ekerdt, J. (2002), "Chemical reactor analysis and design fundamentals", Chapter 7, Madison, Nob Hill Publishing.

Secanell, M., Karan, K., Suleman, A. and Djilali, N. (2007), "Multi-variable optimization of PEMFC cathodes using an agglomerate model", *Electrochimica Acta*, Vol. 52 No. 22, pp. 6318-6337.

Siegel, N.P., Ellis, M.W., Nelson, D.J. and von Spakovsky M.R. (2003), "Single domain PEMFC model based on agglomerate catalyst geometry", *Journal of Power Sources*, Vol. 115 No.1, pp. 81-89.

Song, D., Wang, Q., Liu, Z., Navessin, T., Eikerling, M. and Holdcroft, S. (2004) "Numerical optimization study of the catalyst layer of PEM fuel cell cathode", *Journal of Power Sources*, Vol. 126 No. 1–2, pp. 104-111.

Sun, W., Peppley, B.A. and Karan, K. (2005), "An improved two-dimensional agglomerate cathode model to study the influence of catalyst layer structural parameters", *Electrochimica Acta*, Vol. 50 No. 16–17, pp. 3359-3374.

Tabe, Y., Nishino, M., Takamatsu, H. and Chikahisa, T. (2011), "Effects of Cathode Catalyst Layer Structure and Properties Dominating Polymer Electrolyte Fuel Cell Performance", *Journal of The Electrochemical Society*, Vol. 158 No. 10, pp. B1246-B1254.

Um, S. and Wang, C.Y. (2004). "Three-dimensional analysis of transport and electrochemical reactions in polymer electrolyte fuel cells", *Journal of Power Sources*, Vol. 125 No. 1, pp. 40-51.

Wang, Q., Eikerling, M., Song, D. and Liu, Z. (2004), "Structure and performance of different types of agglomerates in cathode catalyst layers of PEM fuel cells", *Journal of Electroanalytical Chemistry*, Vol. 573, No. 1, pp. 61-69.

Yin, K.M. (2005), "Parametric Study of Proton-Exchange-Membrane Fuel Cell Cathode Using an Agglomerate Model", *Journal of The Electrochemical Society*, Vol. 152 No. 3, pp. A583-A593.

Yoon, W. and Weber, A.Z. (2011), "Modeling Low-Platinum-Loading Effects in Fuel-Cell Catalyst Layers", *Journal of The Electrochemical Society*, Vol. 158 No. 8, pp. B1007-B1018.

Zhou, T. and Liu, H. (2004), "A 3D model for PEM fuel cells operated on reformate", *Journal of Power Sources*, Vol. 138 No. 1–2, pp. 101-110.

Table 1 List of the constants and physical parameters used in the model.

Parameter	Value
Faradays' constant, F	96485 C mol^{-1}
Universal gas constant, R	8.314 J mol^{-1} K^{-1}
Electrochemical surface area of catalyst, A_{pt}	40 m^{2} g^{-1} (Yoon and Weber, 2011)
Temperature, T	353 K
Pressure, p	1.5 atm
Thickness of catalyst layer, L_{cl}	15 µm
Platinum loading, l_{pt}	0.4 mg cm^{-2}
Length of the diffusion path, L_{agg}	1 µm
Thickness of the ionomer film	100 nm
Oxygen diffusivity in the ionomer, D_e	8.45×10^{-10} m^{2} s^{-1} (Sun et al, 2005)
Henry's constant for oxygen in the ionomer, H	0.3125 atm m^{3} mol^{-1} (Sun et al, 2005)
Ionomer volume fraction in the agglomerate, ε_e	0.5
Reference concentration of dissolved oxygen, $C_{O_2}^{ref}$	0.85 mol m^{-3} (Sun et al, 2005)
The gaseous oxygen at the surface of the agglomerate [a]**,** $C_{O_2,g}$	9.18 mol m^{-3}
Exchange current density, i_o	0.015 A m^{-2} (Sun et al, 2005)
Charge transfer coefficient, α	0.61(Sun et al, 2005)

[a] Calculated at 80 °C, 1.5 atm. and 50% relative humidity.

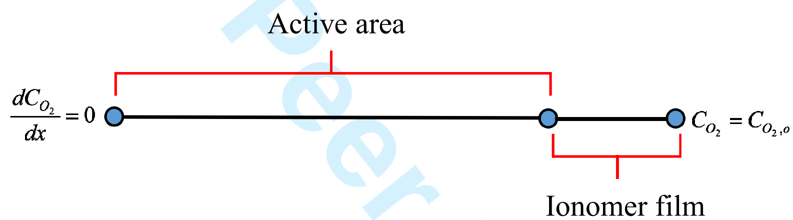

Figure 1. A schematic of the one-dimensional computational domain for the agglomerates investigated.

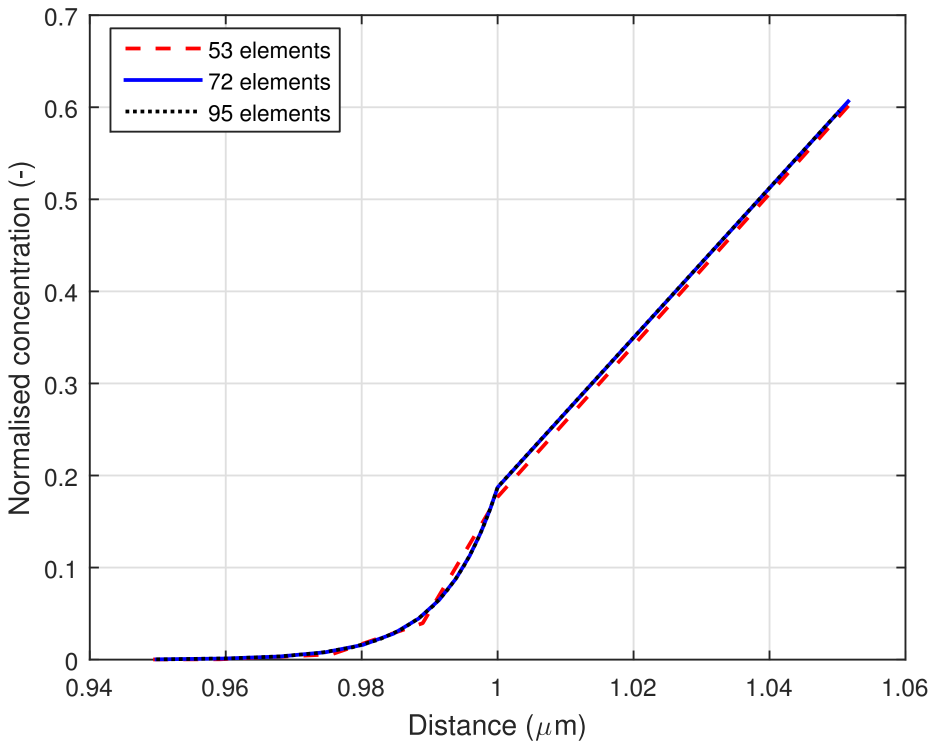

Figure 2. The concentration profiles at -0.8 V over-potential at the interface between the ionomer film and the active region in the slab-like agglomerate for various number of elements. Note that the concentration was normalised to the concentration at the surface of the agglomerate, i.e. 0.85 mol m^{-3}.

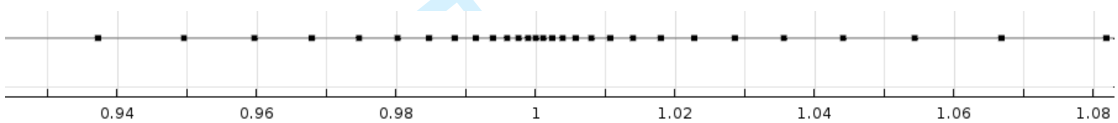

Figure 3. The distribution of the elements in the regions next to the interface between the ionomer film and the active region. The numbers represent the distance in μm.

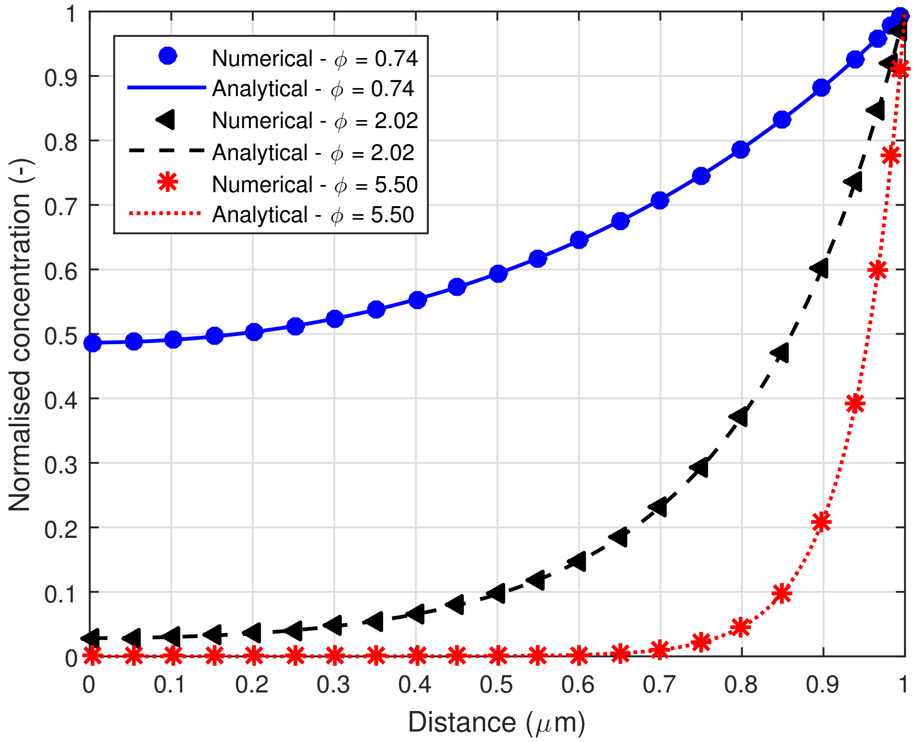

Figure 4. A comparison between the analytical solution and the numerical solution of the concentration profile of the dissolved oxygen within the spherical agglomerate at various Thiele moduli. The Thiele moduli 0.74, 2.02 and 5.50, calculated using Equation (10), are corresponding to over-potentials of -0.4, -0.5 and -0.6 V. The concentration was normalised to the concentration at the surface of the agglomerate, i.e. 0.85 mol m^{-3}.

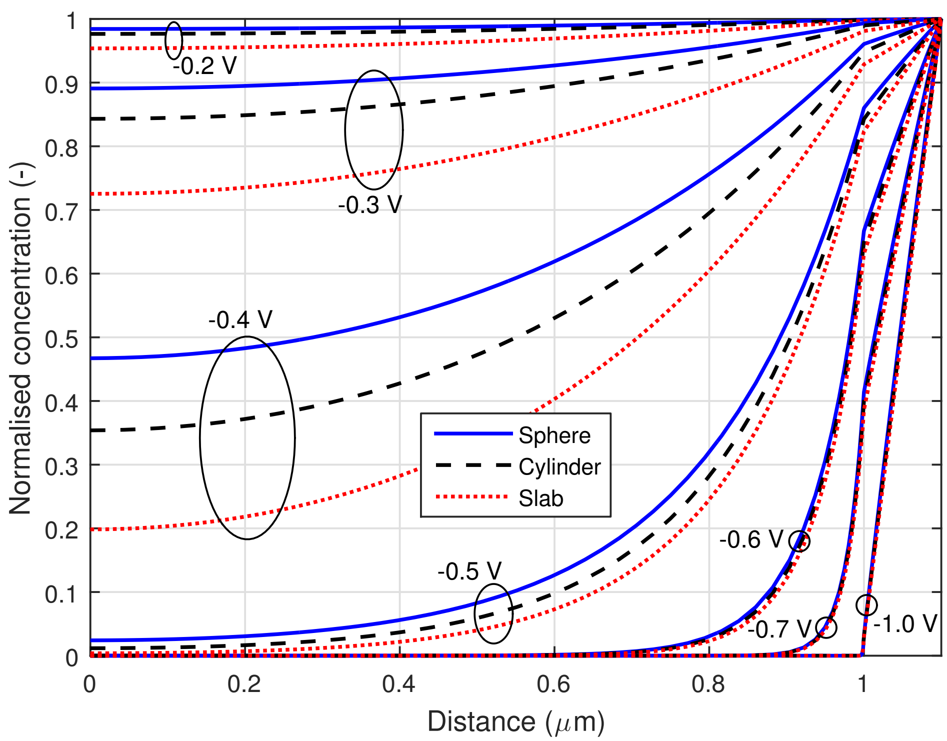

Figure 5. The concentration profiles within the investigated agglomerate at various over-potentials.

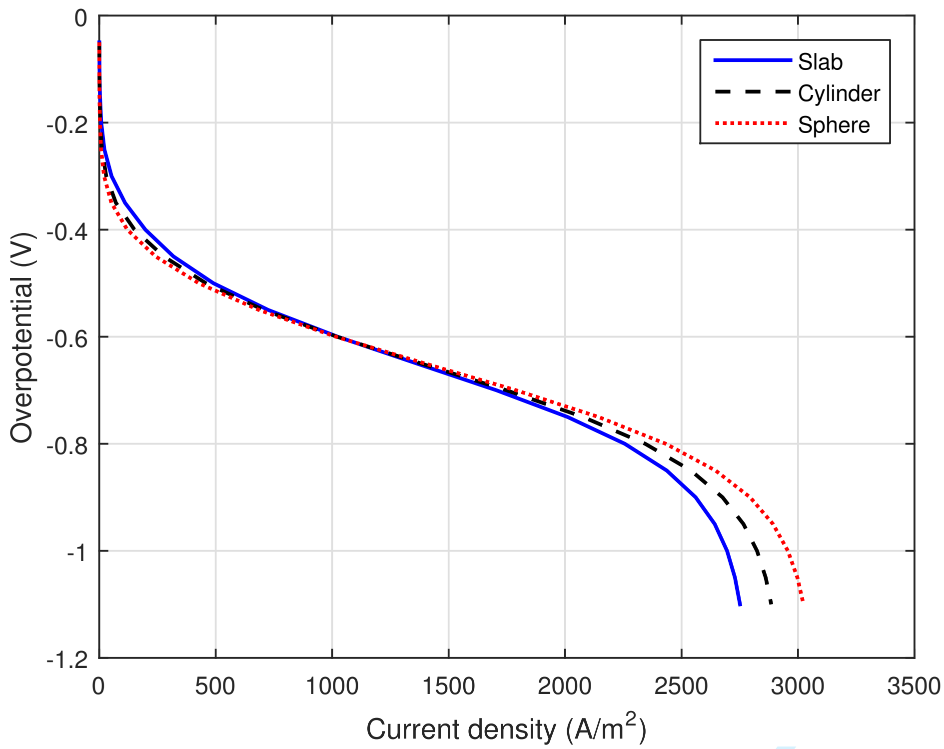

Figure 6. The polarisation curves of the 1D modelled slab-like, cylindrical and spherical agglomerates.